Unusual Solvent Polarity Dependent Excitation Relaxation Dynamics of a Bis[*p*-ethynyldithiobenzoato]Pd-linked Bis[(porphinato)zinc] Complex

Jaehong Park[a,b,c,*], Tae-Hong Park[b,d], Louise E. Sinks[b], Pravas Deria[b,e], Jiyong Park[f], Mu-Hyun Baik[f], and Michael J. Therien[c,*]

a) Department of Molecular Engineering, Graduate School of Engineering, Kyoto University, Nishikyo-ku, 615-8510, Japan.

b) Department of Chemistry, University of Pennsylvania, 231 South 34th Street, Philadelphia, Pennsylvania, 19104-6323, United States.

c) Department of Chemistry, Duke University, French Family Science Center, 124 Science Drive, Durham, North Carolina 27708-0346, United States.

d) Nuclear Chemistry Research Division, Korea Atomic Energy Research Institute, Daejeon, 34057, South Korea.

e) Department of Chemistry, Southern Illinois University, 1245 Lincoln Drive, Carbondale, Illinois 62901, United States.

f) Department of Chemistry, Korea Advanced Institute of Science and Technology (KAIST) & Center for Catalytic Hydrocarbon Functionalizations, Institute for Basic Science (IBS), Daejeon 34141, South Korea.

*To whom correspondence should be addressed:

*Jaehong Park

j.park@moleng.kyoto-u.ac.jp

Tel: +81-75-383-2549; Fax: +81-75-383-2556

*Michael J. Therien

michael.therien@duke.edu

Tel: +2-919-660-1670; Fax: +2-919-684-1522

Experimental Section

Materials. Model compounds (5-triisopropylsilylethynyl-10,20-bis[2',6'-bis(3,3-dimethyl-1-butyloxy)phenyl]porphinato)zinc(II) (**PZnE**)[1] and bis[4-[(3',5'-di-*t*-butylphenyl) ethynyl]dithiobenzoato]palladium(II) (**Ph−Pd(edtb)$_2$−Ph**) were synthesized using previously published methods.[2] [5-Ethynyl-10,20-bis(2',6'-bis(3,3-dimethyl-1-butyloxy)phenyl)porphinato]zinc(II) (**1**)[3], 4-iododithiobenzoic acid 2-(trimethylsilyl)ethyl ester (**2**)[4], and 4-[(3',5'-di-*t*-butylphenyl)ethynyl]dithiobenzoic acid 2-(trimethylsilyl)ethyl ester (**3**) precursors[2], were synthesized via literature methods.

Synthesis of 4-[(10',20'-bis(2',6'-bis(3,3-dimethyl-1-butyloxy)phenyl) porphinato)zinc(II)ethyn-5'-yl]dithiobenzoic acid 2-(trimethylsilyl)ethyl ester (3). Into a Schlenk tube were placed 209 mg of [5-ethynyl-10,20-bis(2'6'-bis(3,3-dimethyl-1-butyloxy)phenyl)porphinato]zinc(II)(**1**, 0.22 mmol), 164 mg of 4-iododithiobenzoic acid 2-(trimethylsilyl)ethyl ester (**2**, 0.43 mmol), and 50 mg of $Pd(PPh_3)_4$ (0.043 mmol). The tube was then evacuated and backfilled with Ar (g) three times. THF/Et_3N (5:1; 10 mL), deaerated by 3 cycles of freeze-pump-thaw-degas cycles, was added to the tube, which was then heated at 45 °C under Ar (g) for 24 h. The mixture was diluted in 10 mL of CH_2Cl_2 and washed twice with saturated NH_4Cl (aq) and water. The combined aqueous layers were twice extracted with CH_2Cl_2, and the combined organic layers were dried over $MgSO_4$. After the solvent was evaporated, the residue was chromatographed on silica gel using 10% THF in hexanes as eluent to afford **3**. The product was further purified by recrystallization in CH_2Cl_2/hexanes (228 mg, 88 % yield based on **1**). ^{1}H NMR ($CDCl_3$, 500 MHz): δ 10.07 (1H, s), 9.75 (2H, d, J = 4.6 Hz), 9.23 (2H, d, J = 4.4 Hz), 8.99 (2H, d, J = 4.6 Hz), 8.93 (2H, d, J = 4.4 Hz), 8.22 (2H, d, J = 8.3 Hz), 8.01 (2H, d, J = 8.4 Hz), 7.72 (2H, t, J = 8.5 Hz), 7.02 (4H, d, J = 8.5 Hz), 3.91 (8H, t, J =

7.2 Hz), 3.45 (2H, m), 1.10 (2H, m), 0.85 (8H, m), 0.21 (36 H, s), and 0.15 (9H, s) ppm. IR (film, KBr disk): 3445, 3088, 2953, 2863, 2186, 1590, 1501, 1455, 1384, 1364, 1332, 1307, 1239, 1210, 1180, 1097, 1059, 1045, 999, 946, 899, 835, 793, 765, and 715 cm^{-1}. UV-vis (log ε_{abs}, in THF): 319 (4.41), 431 (5.11), 445 (5.20), 569 (4.19), and 627 (4.53) nm; (log ε_{abs}, in $CHCl_3$): 318 (4.43), 442 (5.23), 564 (4.25), 614 (4.38), and 625 (4.35) nm. MALDI-TOF calcd for $C_{70}H_{84}N_4O_4S_2SiZn$ $(M)^+$: 1200.50, found 1200.93. Anal. calcd for $C_{70}H_{84}N_4O_4S_2SiZn$: C 69.89%, H 7.04%, N 4.66%, found C 69.58%, H 6.73%, N 4.62%.

Synthesis of Bis[4-[(10',20'-bis(2',6'-bis(3,3-dimethyl-1-butyloxy)phenyl) porphinato)zinc(II)ethyn-5'-yl]dithiobenzoato]palladium(II) (PZn−Pd(edtb)$_2$−PZn). A 0.1 M TBAF solution (0.60 mL, 60.0 μmol) was added to **3** (47.9 mg, 39.8 μmol) in THF (4 mL). After 20 min, the solvent was evaporated and dried under vacuum for 15 min, and the residue was then dissolved in $CHCl_3$. A MeOH solution (12.4 mM) of $PdCl_2$ (1.5 mL, 19.0 μmol) was added to the porphyrin solution and the mixture was stirred for 30 min. The precipitate was filtered and washed with acetone and MeOH to afford analytically pure solid **PZn−Pd(edtb)$_2$−PZn** (38 mg, 83% yield based on $PdCl_2$). ^{1}H NMR (THF-d_8, 500 MHz): δ 9.96 (2H, s), 9.68 (4H, d, J = 4.5Hz), 9.13 (4H, d, J = 4.3 Hz), 8.89 (4H, d, J = 4.4 Hz), 8.78 (4H, d, J = 4.3 Hz), 8.32 (4H, d, J = 8.1 Hz), 8.18 (4H, d, J = 8.18 Hz), 7.73 (4H, t, J = 8.6 Hz), 7.11 (8H, d, J = 8.6 Hz), 3.96 (16H, t, J = 7.6 Hz), 0.78 (16H, m), and 0.41 (72H, s) ppm. IR (film, KBr disk): 3115, 3082, 12953, 2863, 3182, 1590, 1521, 1499, 1456, 1385, 1365, 1335, 1303, 1261, 1241, 1209, 1171, 1098, 1098, 1057, 997 (CSS), 944 (CSS), 838, 790, 764, and 714 cm^{-1}. UV-vis (THF, log ε_{abs}): 330 (4.76), 427 (5.53), 544 (4.79), and 687(5.02) nm. MALDI-TOF calcd for $C_{130}H_{142}N_8O_8PdS_4Zn_2$ (M^+): 2304.75, found 2307.85. Anal.

calcd for $C_{130}H_{142}N_8PdO_8S_4Zn_2$: C 67.59%, H 6.20%, N 4.85%, found C 67.34%, H 5.93 %, N 4.59%.

Instrumentation. FT-IR spectra were obtained using a PerkinElmer Spectrum 100 FT-IR Spectrometer. The samples were prepared as a translucent film on a KBr disk (Aldrich) by drop-casting from a concentrated $CHCl_3$ solution. NMR spectra were recorded on a 500 MHz AMX-500 Brüker spectrometer. Chemical shifts for ^1H spectra were referenced to the residual solvent peak. MALDI-TOF mass spectroscopic data were obtained with a Perspective Voyager DE instrument in the Laboratory of Professor William DeGrado (Department of Biophysics, University of Pennsylvania). Elemental analysis data were acquired at Robertson Microlit Laboratories (Madison, NJ).

Time-Resolved Emission Experiments. Magic-angle polarization time-resolved emission decay data were recorded using a Hamamatsu C4780 picosecond fluorescence lifetime measurement system. It utilizes a Hamamatsu Streakscope C4334 as photoncounting detector, and a Hamamatsu C4792-01 synchronous delay generator and a Stanford Research Systems DG535 serve as electronic delay generators. The samples were excited either by Hamamatsu PLP-10 laser diode (650 nm) or by femtosecond laser pulse generated by the following description; optical pulses ($\geq$ 120 fs) centered at 780 nm were generated using a Ti:Sapphire laser (Clark-MXR, CPA-2001, Dexter, MI, USA), which consists of a regenerative amplifier seeded by a mode-locked fiber oscillator, and the output of regenerative amplifier feeds a optical parametric amplifier (Light Conversion, TOPAS-C, Lithuania) which generates excitation pulses tunable in wavelength from the UV through the NIR region. The polarization and attenuation of the femtosecond laser pump pulse were controlled by a half-wave plate and Rochon prism polarizer pairs and the polarization of emission was set to the magic

angle (54.7 °) for these experiments. Hamamatsu HPD-TA software was used to acquire emission data in the single-photon counting mode. Deconvolution of these data utilized a scattering sample (cream dissolved in water) to acquire the instrument response function. Sample concentrations were adjusted to give an optical density of ~0.1 at the excitation wavelength.

Nanosecond Transient Absorption Experiments. The nanosecond transient absorption spectra were collected from LP920 spectrometry system from Edinburgh Instruments, based on the nanosecond flash photolysis technique. A pump pulse was generated in the way that Q-switched Nd:YAG laser (Quantel, Brilliant, Bozeman, MT, USA) injected into optical parametric oscillator (OPO) (OPOTEK, Vibrant, Carlsbad, CA, USA) to tune the wavelength. The pulse width of the pump was c.a. 5ns, and the pulse energy was controlled to be ~1.5 mJ/pulse, and a Xe flash-lamp was used as a white light probe source. An ICCD camera (AndoriStar) was used to acquire data over the 185-to-870 nm spectral domain. The LP920 and OPO were computer interfaced and controlled. The spectra were averaged over ~5-20 repetitions. Samples were prepared in 1 cm quartz cells and were degassed by five successive freeze-pump-thaw-degas cycles. Excited-state lifetimes were calculated by performing an exponential fitting at the decay or the ground-state bleach rise wavelength using Origin 7.5 software.

Ultrafast Transient Absorption Experiments. Ultrafast transient absorption spectra were obtained using standard pump-probe methods. Optical pulses (≥ 120 fs) centered at 780 nm, were generated using a Ti:Sapphire laser (Clark-MXR, CPA-2001, Dexter, MI, USA), which consisted of a regenerative amplifier seeded by a mode-locked fiber oscillator. The output of regenerative amplifier was split to feed a home-built optical parametric amplifier (OPA), which generates excitation pulses tunable in

wavelength from the UV through the NIR region. The pump beam was chopped at half the laser repetition rate (~500 Hz). A fraction (< 5%) of the output from the regenerative amplifier was passed through an optical delay line, and focused onto a 2 mm c-cut sapphire plate to generate a white light continuum, which was used as the probe beam. The polarization and attenuation of the pump and probe beams were controlled by a half-wave plate and Rochon prism polarizer pairs. The polarization was set to the magic angle (54.7 °) for these experiments. The pump beam was focused into the sample cell with an f = 20 cm lens, while the probe beam was focused with a concave mirror. The spot size diameter was 0.2−0.3 mm. The beam diameter was determined using the razor-blade method. The excitation pump power was measured using a power meter (Coherent, LabMax Top with PS19 head). After passing through the sample, the probe light was adjusted using a neutral density filter to avoid saturating the detectors, and focused onto the entrance slit of a computer-controlled image spectrometer (Acton Research Corporation, SpectraPro-150, Trenton, NJ, USA). A CCD array detector (1024 x 128 elements, Roper Scientific, Trenton, NJ, USA), interfaced to the spectrometer, recorded the spectrum of the probe light from the UV (~370 nm) to the NIR (~1100 nm), providing spectral resolution better than 0.5 nm. Transient absorption data acquired over 0.9-1.4 μm NIR region were recorded using a liquid nitrogen cooled InGaAs 512-element linear array detector (Roper Scientific, Trenton, NJ, USA) interfaced to a SpectraPro-2150 spectrometer. Pairs of consecutive spectra were measured with ($I_{on}(\lambda)$) and ($I_{off}(\lambda)$) to determine the difference spectrum, $\Delta A = \log(I_{off}(\lambda)) / (I_{on}(\lambda))$. All these experiments utilized a custom-built 2 mm-path-length fused-silica sample cell; all transient optical studies were carried out at 20 ± 1 °C. All transient spectra reported represent averages obtained over 3-5 scans, with each scan

consisting of 1000-2000 frames with ~100-200 data points. In these experiments, the delay line utilizes a computer-controlled delay stage. Delay times up to 6 ns were achieved using a Compumotor-6000 (Parker). The baseline noise level in these transient absorption experiments corresponded to ~ 0.2 mOD per second of signal accumulation. The time resolution is probe wavelength dependent; in these experiments, the FWHM of the instrument response function (IRF) varied between 140–200 fs (*e.g.*, at 680 nm, the IRF was 150 ± 6 fs). Following all pump-probe transient absorption experiments, electronic absorption spectra verified that the sample solutions were robust.

Quantum Yield Calculation of Triplet State Formation (Φ_T). The population of excited lowest triplet-state (T_1) after the excitation to S_1 is expressed as equation (S1):[5]

$$[\mathrm{E}]_{\mathrm{T1,t}} = [\mathrm{E}]_{\mathrm{S1,t=0}}\Phi_{\mathrm{T}}[1 - \exp(-kt)] \qquad \text{(S1)}$$

where $[E]_{T1,t}$ is the population of T_1 state $t_{delay} = t$, $[E]_{S1,t=0}$ is the population of S_1 at $t_{delay} = 0$, Φ_T is the quantum yield of triplet-state formation ($S_1 \rightarrow T_1$), and k is the depopulating rate constant of S_1-state through $S_1 \rightarrow S_0$, $S_1 \rightarrow S^*$ relaxation, and $S_1 \rightarrow T_1$ intersystem crossing processes. When $t >> (1/k)$, $\exp(-kt) \rightarrow 0$, and therefore, Φ_T can be rewritten as the following (S2);

$$\Phi_{\mathrm{T}} = \frac{[\mathrm{E}]_{\mathrm{T1,t}}}{[\mathrm{E}]_{\mathrm{S1,t=0}}} \qquad \text{(S2)}$$

To obtain the population of excited states in transient absorption spectra, the following calculation is necessary. For a four-state model (ground (G), S_1, S^*, and T_1), the absorbance of a sample, A_0, at wavelength λ is given by the Beer's Law.

$$\mathrm{A}_0(\lambda) = \varepsilon_{\mathrm{g}}(\lambda)[\mathrm{G}]_0 l \qquad \text{(S3)}$$

where $\varepsilon_g(\lambda)$ is the extinction coefficient of the ground state at wavelength λ, $[G]_0$ is the total concentration of a sample, and l is the beam path length. The absorbance of a sample after excitation, A_1, at wavelength λ at a delay time t, is given by

$$A_1(\lambda, t) = A_1^G(\lambda, t) + A_1^E(\lambda, t) \quad \text{(S4)}$$

where $A_1^G(\lambda, t)$ and $A_1^E(\lambda, t)$ is the absorption contribution at t_{delay} from the remaining ground state population, and from the excited state population, respectively, at wavelength λ. Here, $[E]_t$ is given by the following relation;

$$[E]_t = [E]_{t,S1} + [E]_{t,S*} + [E]_{t,T1} = [G]_0 - [G]_t \quad \text{(S5)}$$

where $[G]_t$ is the population in the ground state at t_{delay}. Difference absorbance (ΔA) is expressed as described in equation (S6), using eq (S5).

$$\Delta A_1(\lambda, t) = A_1(\lambda, t) - A_0(\lambda) = A_1^G(\lambda, t) + A_1^E(\lambda, t) - A_0(\lambda)$$

$$= A_1^E(\lambda, t) - \varepsilon_g(\lambda)[E]_t l \quad \text{(S6)}$$

Eq (6) is valid only if stimulated emission (SE) is negligible at λ, which is not the case of our data where we monitor the wavelength (λ_B) for bleaching bands. To account for the contribution from stimulated emission (SE), eq (S6) is modified.

$$\Delta A_1(\lambda, t) = A_1^E(\lambda, t) - \varepsilon_g(\lambda)[E]_t l - SE(\lambda, t) \quad \text{(S7)}$$

where $SE(\lambda,t)$ is the intensity of SE in λ at the t_{delay}. In **PZn−Pd(edtb)$_2$−PZn**, since the decay rates in the singlet state manifolds ($S_1 \rightarrow S_0$ and $S^* \rightarrow S_0$) are much faster than that of the triplet state, we can assume at the end of our time delay (3 ns), all the excited population reside in the triplet state, thus $[E]_{t=3ns,S1} + [E]_{t=3ns,S*} \approx 0$. In addition, since the T_1-state lifetime (τ_T) of **PZn−Pd(edtb)$_2$−PZn** is ~2−3 μs, the T_1-state depopulation during the initial 3 ns is assumed to be negligible.

$$[\mathrm{E}]_{\mathrm{t=3ns}} \approx [\mathrm{E}]_{\mathrm{T1}} \qquad \text{(S8)}$$

$$\Delta \mathrm{A}_1(\lambda, 3\mathrm{ns}) = \mathrm{A}_1^{\mathrm{E}}(\lambda, 3\mathrm{ns}) - \varepsilon_{\mathrm{g}}(\lambda)[\mathrm{E}]_{\mathrm{t=3ns}} l. \qquad \text{(S9)}$$

For **PZn−Pd(edtb)$_2$−PZn**, two relaxation mechanisms ($S_1 \rightarrow T_1 \rightarrow S_0$ and/or $S_1 \rightarrow S^* \rightarrow S_0$) play roles of varying importance depending on solvent polarity; excited-population depletion during the first 5 ps is assumed to be negligible, based upon the lifetimes of S* ($\tau_{S^*} \approx 70-200$ ps) and T_1 ($\tau_T \approx 2-3$ μs) states. Therefore, it is assumed that $[E]_{t=5ps} \approx [E]_{t=0}$, and the $[E]_{t=0}$ can be obtained from below eq (S10):

$$\Delta \mathrm{A}_1(\lambda, 5\mathrm{ps}) = \mathrm{A}_1^{\mathrm{E}}(\lambda, 5\mathrm{ps}) - \varepsilon_{\mathrm{g}}(\lambda)[\mathrm{E}]_{\mathrm{t=5ps}} l \approx \mathrm{A}_1^{\mathrm{E}}(\lambda, 5\mathrm{ps}) - \varepsilon_{\mathrm{g}}(\lambda)[\mathrm{E}]_{\mathrm{t=0}} l \qquad \text{(S10)}$$

From eq (S2), (S9), and (S10), the Φ_T can be calculated as below.

$$\Phi_{\mathrm{T}} = \frac{[\mathrm{E}]_{\mathrm{T1,t=3ns}}}{[\mathrm{E}]_{\mathrm{t=0}}} = \frac{[\mathrm{E}]_{\mathrm{t=3ns}}}{[\mathrm{E}]_{\mathrm{t=5ps}}}$$

$$= \frac{[\mathrm{A}_1^{\mathrm{E}}(\lambda, \mathrm{t_{delay}=3ns}) - \Delta \mathrm{A}_1(\lambda, \mathrm{t_{delay}=3ns})]}{[\mathrm{A}_1^{\mathrm{E}}(\lambda, \mathrm{t_{delay}=5ps}) - \Delta \mathrm{A}_1(\lambda, \mathrm{t_{delay}=5ps})]} \qquad \text{(S11)}$$

Note that $\mathrm{A}_1^{\mathrm{E}}(\lambda, t)$ is an extrapolated value as described in the previous literature.[6]

Details of the Computational Methods. Conformational preferences of the **PZn−Pd(edtb)$_2$−PZn** was analyzed by means of density functional theory calculations. The geometry of the planar (**Fig. S3a**) and the perpendicular conformations were optimized at the B3LYP/LACVP** level of theory, which is equivalent to B3LYP/6-31G(d,p)/LANL2DZ level of theory. Single point electronic energies were computed at the triple zeta quality basis sets, namely B3LYP/cc-pVTZ(-f)/LACV3P level of theory. Effective core potentials (ECP) were employed for the transition metals (Zn and Pd). We used Jaguar v9.1 software for the computations.[7] The coordinate scans were computed at the B3LYP/LACVP** level of theory. The relative angles (θ_1 and θ_2 in **Fig. S3b**) of the molecular fragments were restrained at a designated value, while optimizing

the remaining degrees of freedoms of the molecule. Electronic energies (E_{SCF}) of the optimized geometries at certain relative angles were reported in **Fig. S3b**.

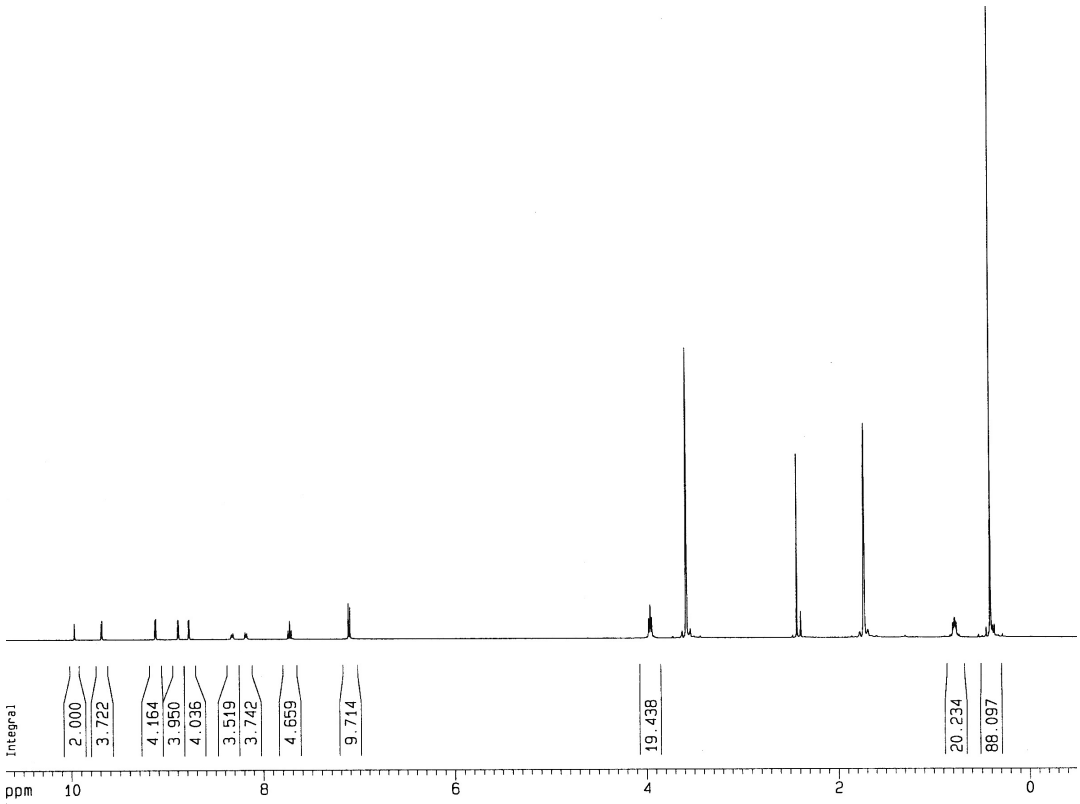

Figure S1. ^{1}H NMR spectrum of **PZn−Pd(edtb)$_2$−PZn** in THF-d_8.

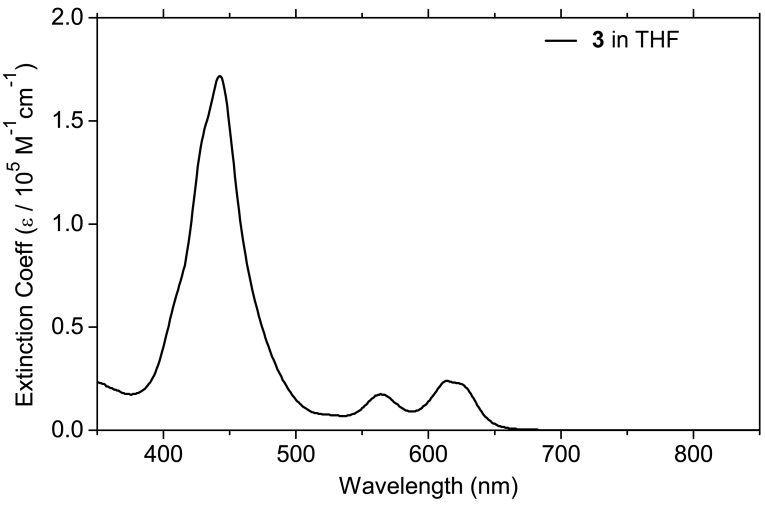

Figure S2. Electronic absorption spectrum of ligand precursor **3** in THF.

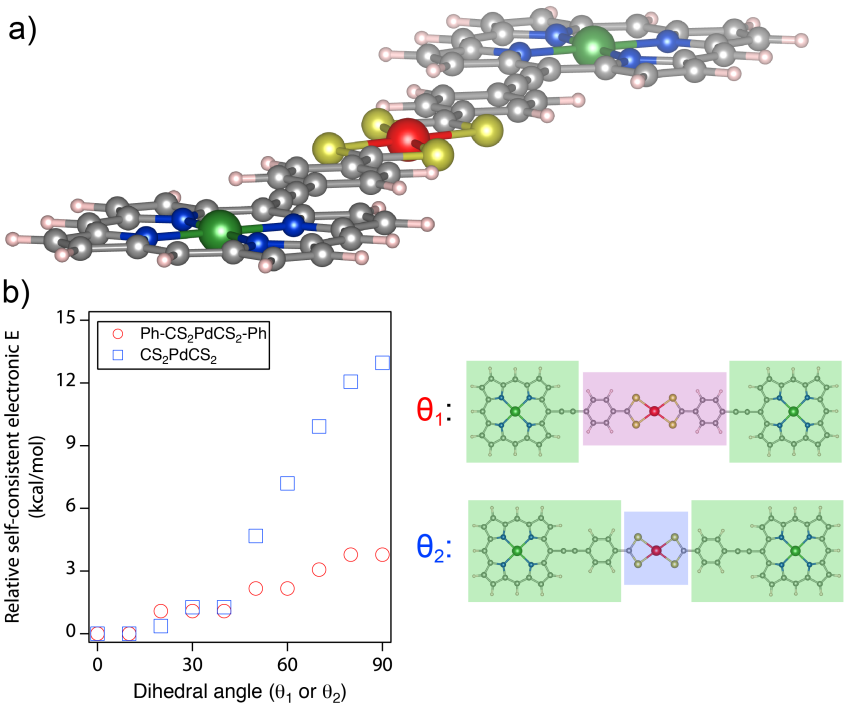

Figure S3. a) The optimized structure of **PZn−Pd(edtb)$_2$−PZn** determined from DFT calculations carried out at the B3LYP level. b) The energetics as a function of dihedral angle (θ_1 or θ_2) between the 5-ethynylporphyrin plane (green color) and the bis(dithiobenzoato)Pd(II) (red color) or the 5-phenylethynylporphyrin plane (green color) and the bis(dithioate)Pd(II) plane (blue color) for θ_1 and θ_2, respectively. The computational analysis showed that the electronic energy of the perpendicular conformer, namely the bis(dithiobenzoato)Pd(II) plane is 90 degree to that of the porphyrin plane, is +4 kcal/mol, which is equivalent to +~0.17 eV. The finding suggests that a substantial population of conformers having modest porphyrin-bridge-porphyrin interplanar torsional angles at ambient temperature.

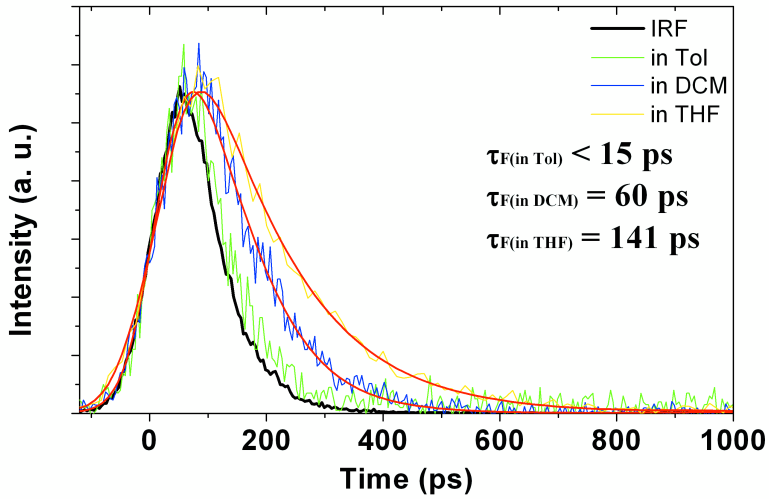

Figure S4. Magic angle time-resolved fluorescence data and corresponding fitting results of **PZn−Pd(edtb)$_2$−PZn** in multiple solvents. A single exponential decay fitting convoluted with an instrumental response function determines fluorescence lifetimes to be <15 ps, 60 ps, and 141 ps in Tol, DCM, and THF, respectively. Experimental conditions: temperature = 20 °C; λ_{ex} = 650 nm.

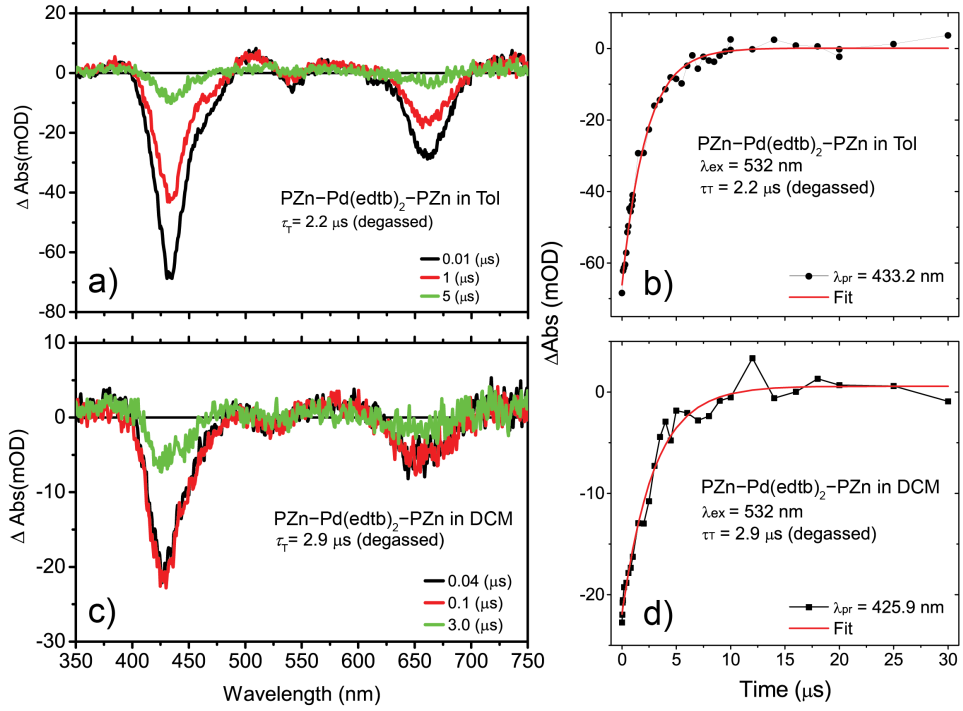

Figure S5. (a,c) Nanosecond transient absorption spectra and (b,d) ground-state bleach recovery profiles of **PZn−Pd(edtb)$_2$−PZn** in degassed (a,b) toluene and (c,d) DCM. Experimental conditions: temperature = 20 °C; λ_{ex} = 532 nm; pump energy = 1.5 mJ/pulse. Single-exponential fits of the data are displayed as solid red lines.

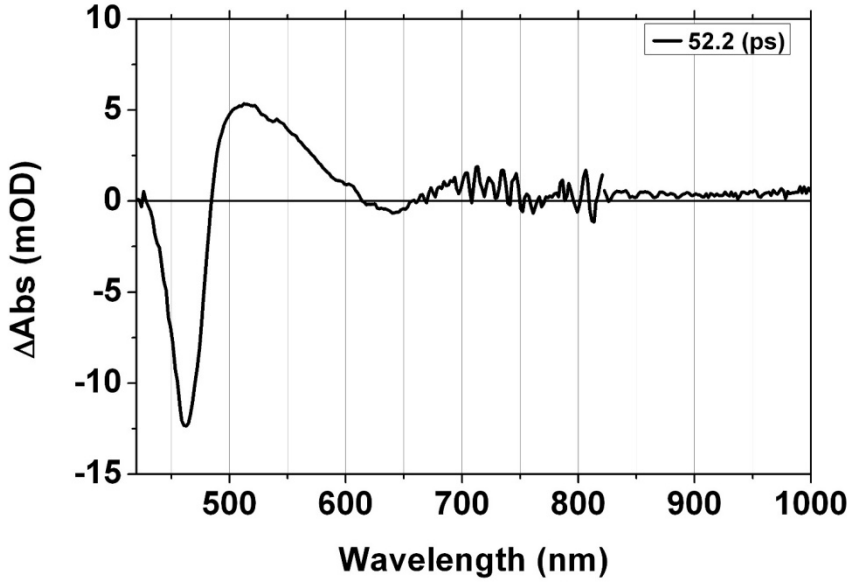

Figure S6. Magic angle femtosecond transient absorption spectra of **Ph−Pd(edtb)$_2$−Ph** in toluene, recorded at the time delay of 52 ps. Experimental conditions: temperature = 20 °C; λ_{ex} = 388 nm; pump energy = 700 nJ/pulse.

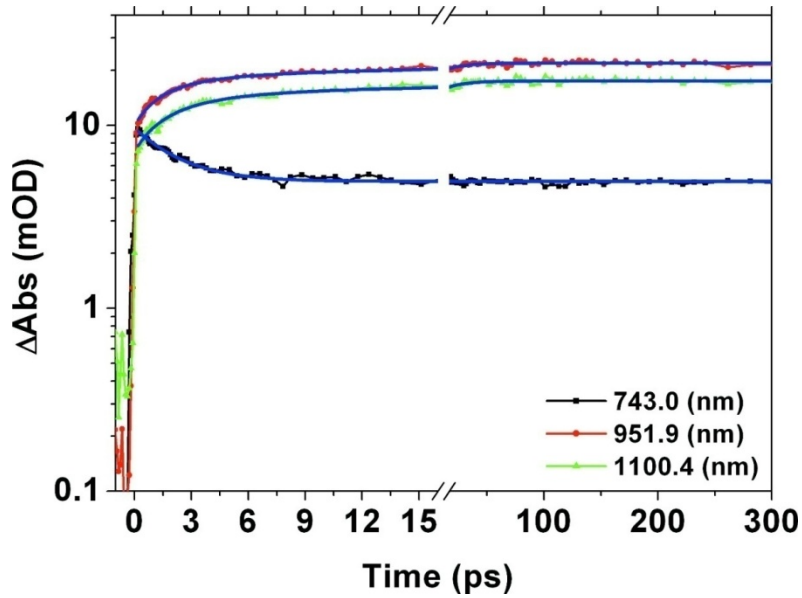

Figure S7. Exemplary wavelength-dependent transient decays obtained for **PZn−Pd(edtb)$_2$−PZn** in Tol. A multiwavelength fit of the data, using three exponential functions, gives τ_1= 2.0 ps, τ_2= 16 ps, τ_3> 3 ns (long component), which are depicted by thin lines. Experimental conditions: λ_{ex}= 650 nm; pulse energy = 300 nJ/pulse; temperature = 20 °C; magic angle polarization.

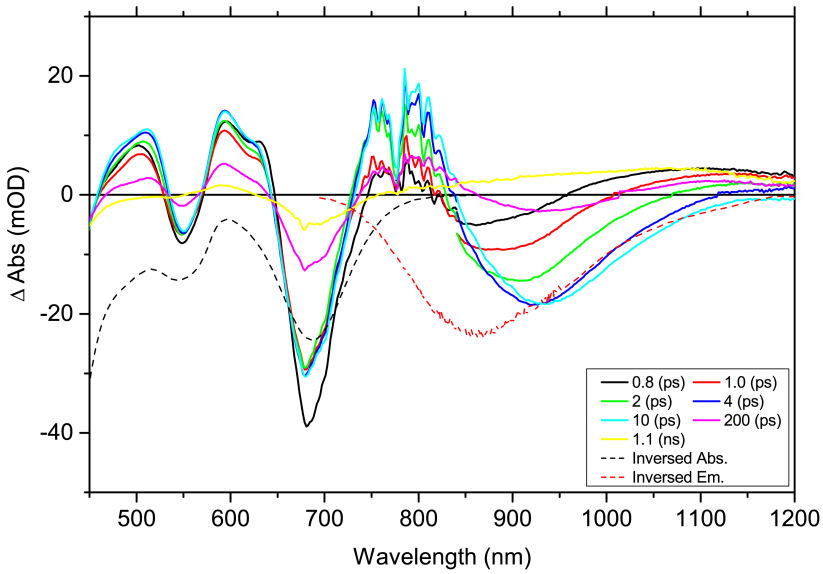

Figure S8. Representative fs-TA spectra of **PZn−Pd(edtb)$_2$−PZn** in THF, recorded at time delays noted. Experimental conditions: temperature = 20 °C; λ_{ex} = 671 nm; pump energy = 0.5 μJ/pulse; magic angle polarization. Inversed steady-state absorption (black dashed line) and emission spectra (red dashed line) are displayed for comparison.

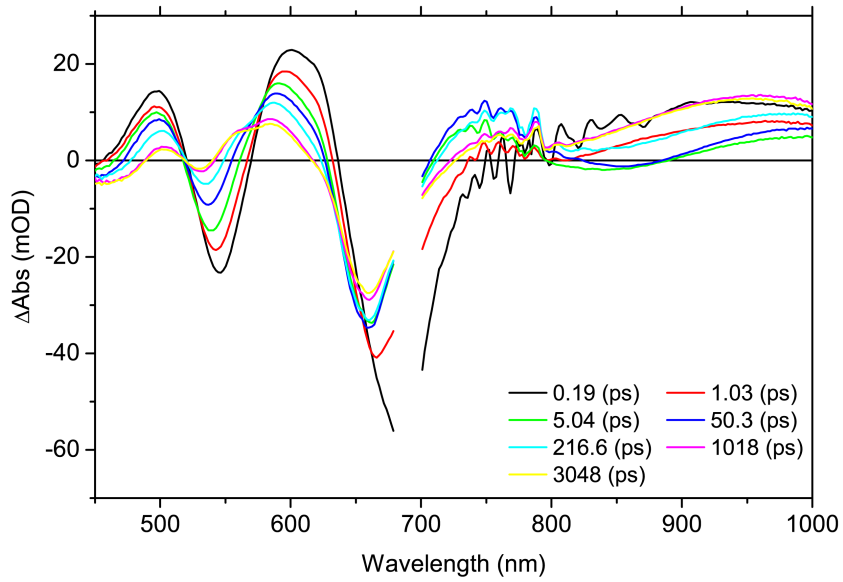

Figure S9. Representative fs-TA spectra of **PZn−Pd(edtb)$_2$−PZn** in DCM/Tol (χ_{mol} = 0.40), recorded at time delays noted. Experimental conditions: temperature = 20 °C; λ_{ex} = 690 nm; pump energy = ~0.5 μJ/pulse; magic angle polarization.

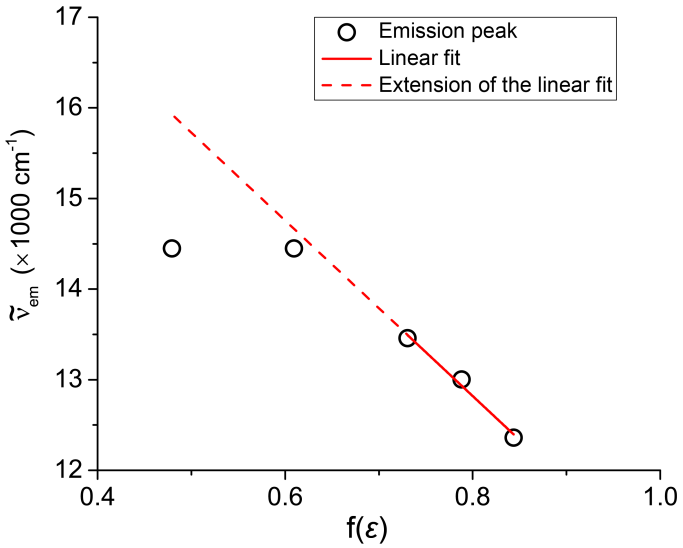

Figure S10. Steady-state emission peak position ($\tilde{\nu}_{em}$) as a function of Onsager function ($f(\varepsilon)$ = 2(ε–1)/(2ε+1)) obtained for **PZn−Pd(edtb)$_2$−PZn** in DCM/Tol mixture. The linear fit for χ_{mol} = 0.40, 0.62, and 1.0 is shown in a red solid line, whereas the predicted extension of the corresponding linear fit is shown in a red dashed line. Since the ε of DCM/Tol mixture is not available, the ε of various χ_{mol} is calculated from $\varepsilon(\chi_{mol})$ = $\chi_{mol}\varepsilon$(DCM) + (1–χ_{mol})ε(Tol).

Table S1. Electronic absorption spectral data of **PZn−Pd(edtb)$_2$−PZn** relative to appropriate chromophoric benchmarks **3** and **Ph−Pd(edtb)$_2$−Ph** in multiple solvents.

Compounds	Sol	Absorption band maxima [nm] ($\varepsilon_{abs}\times 10^{-5}$ [$M^{-1}cm^{-1}$])
PZn−Pd(edtb)$_2$−PZn	Toluene	427 (2.92), 534 (0.82), 652 (1.13)
	DCM	423 (2.82), 523 (0.76), 645 (0.94)
	THF	427 (3.39), 544 (0.61), 687 (1.04)
PZnE[a)]	THF	430 (2.92), 563 (0.12), 606 (0.07)
3	THF	445 (1.58), 569 (0.15), 625 (0.34)
Ph−Pd(edtb)$_2$−Ph	DCM	451 (0.93), 555 (0.03)

a) Electronic absorption data of PZnE are obtained from Ref. 1.

References

1. K. Susumu and M. J. Therien, *J. Am. Chem. Soc.*, 2002, **124**, 8550-8552.
2. T.-H. Park, PhD Dissertation, University of Pennsylvania, 2008.
3. H. T. Uyeda, Y. Zhao, K. Wostyn, I. Asselberghs, K. Clays, A. Persoons and M. J. Therien, *J. Am. Chem. Soc.*, 2002, **124**, 13806-13813.
4. T.-H. Park and M. J. Therien, *Org. Lett.*, 2007, **9**, 2779-2782.
5. H. Hirano and T. Azumi, *Chem. Phys. Lett.*, 1982, **86**, 109-112.
6. T. V. Duncan, I. V. Rubtsov, H. T. Uyeda and M. J. Therien, *J. Am. Chem. Soc.*, 2004, **126**, 9474-9475.
7. A. D. Bochevarov, E. Harder, T. F. Hughes, J. R. Greenwood, D. A. Braden, D. M. Philipp, D. Rinaldo, M. D. Halls, J. Zhang and R. A. Friesner, *Int. J. Quantum Chem*, 2013, **113**, 2110-2142.